Electron correlation in the lanthanides: $4f^2$ spectrum of Ce^{2+}

Charlotte Froese Fischer[*]

Department of Computer Science, University of British Columbia, 2366 Main Mall, Vancouver, British Columbia, Canada V6T 1Z4

Michel R. Godefroid

Chimie Quantique et Photophysique, Université Libre de Bruxelles, CP 160/09, 1050 Brussels, Belgium

Atoms and ions of lanthanides have multiple opens shells along with an open $4f^k$ subshell. This paper studies the effect of electron correlation in such systems and how wave functions can be determined for the accurate prediction of atomic properties in the case of Ce^{2+} where $k = 2$, using the multireference single- and double-excitation method. An efficient higher-order method is recommended for more reliable results.

I. INTRODUCTION

Lanthanides were detected recently in the electromagnetic counterpart to a gravitational wave source from a binary neutron star merger (GW170817) [1]. Knowledge of their atomic structure is essential for estimating the ejecta opacity and understanding the r nuclear process at the origin of their synthesis [2,3]. Lanthanides and related actinides are also the elements of the Periodic Table that pave the way to the transfermium elements ($Z \geqslant 100$) that do not occur naturally on earth and are produced at large accelerator facilities, for which the atomic structure is almost unknown [4], and to superheavy elements ($Z \geqslant 104$) that are good candidates for the island of stability of nuclear astrophysics interest [5].

To estimate the r-process opacities that are dominated by bound-bound transitions, the radiative transition rates have to be calculated for tens of millions of lines in lanthanide ions, using atomic structure models that determine the approximate ion energy-level structure and the wavelengths and oscillator strengths of all permitted radiative transitions [6]. Although these models do not provide exact results, the hope is that they capture the statistical distribution of levels and lines to derive reliable estimates of the pseudocontinuum opacity [7]. Benchmark calculations for a few elements have been performed [8] to confirm that the opacities from bound-bound transitions of open f-shell elements are higher than those of the other elements over a wide wavelength range. The present work does not consider this category of calculations. It mainly focuses on the search of the relevant correlation configurations entering in the description of atomic energy levels of complex atomic systems and to the development of *ab initio* computational strategies allowing their efficient inclusion. The ultimate goal is to improve the reliability of theoretical atomic energy levels, excitation energies, and wave-function compositions, in line with other recent works [9,10].

Parametric studies can be performed to unravel the complex spectra of lanthanides (and actinides) (see, for instance, [11] for Ce^{2+}) but needed are the observed atomic line frequencies and intensities, which are precisely the targets of *ab initio* approaches. The effect of correlation in atoms and ions of lanthanides and actinides is not well understood. Safronova *et al.* [12] summarize the situation well: "Though tremendous progress has been made, calculations for the lanthanides with the open $4f$ shell remain a challenge". In their paper, they report results from applying two hybrid approaches to the elements La, La^+, Ce, Ce^+, Ce^{2+}, and Ce^{3+}. In their studies, not all levels of a configuration are included. In particular, in Ce^{2+} ($Z = 58$) only five levels were reported, namely, $^3H_{4,5,6}$, $^1G_4$, and $^1D_2$, instead of the 13 levels arising from a single-open-subshell f^2 configuration [13]. Their method is based on the use of an effective Hamiltonian for including correlation within the closed subshells and configuration interaction for electrons in open subshells (referred to as valence electrons) and perturbation theory methods of various orders.

The present paper discusses similar strategies based on variational methods for determining wave functions that can be used to predict atomic properties and not only energies, methods that have been implemented in the general relativistic atomic structure package computer codes (GRASP2K [14] and GRASP2018 [15]). What makes the calculations challenging is the rapid explosion in the number of basis states associated with configurations with multiply occupied subshells with large angular momenta and the need for higher-order corrections. The configuration $[Kr]4d^84f^45s^25p^45d^2$ of Ce^{2+} has associated with it 1 608 502 basis states, for $0 \leqslant J \leqslant 6$.

In addition, strong interactions require treatments for higher-order effects and standard procedures rapidly produce expansions of 10×10^6 basis states or more. Once wave functions have been determined, other properties can be computed.

II. UNDERLYING THEORY

In the multiconfiguration Dirac-Hartree-Fock (MCDHF) method [16], the wave function $\Psi(\gamma \pi JM_J)$ for a state labeled $\gamma \pi JM_J$, where J and M_J are the angular quantum numbers

*cff@cs.ubc.ca

and π is the parity, is expanded in antisymmetrized configuration state functions (CSFs)

$$\Psi(\gamma \pi J M_J) = \sum_{j=1}^{N} c_j \Phi(\gamma_j \pi J M_J). \tag{1}$$

The label $\{\gamma_j\}$ denotes other appropriate information about the CSFs, such as orbital occupancy and the subshell coupling tree. The CSFs are built from products of one-electron orbitals, having the general form

$$\psi_{n\kappa,m}(\mathbf{r}) = \frac{1}{r}\begin{pmatrix} P_{n\kappa}(r)\chi_{\kappa,m}(\theta,\varphi) \\ iQ_{n\kappa}(r)\chi_{-\kappa,m}(\theta,\varphi) \end{pmatrix}, \tag{2}$$

where $\chi_{\pm\kappa,m}(\theta,\varphi)$ are two-component spin-angular functions. The radial functions $\{P_{n\kappa}(r), Q_{n\kappa}(r)\}$ are represented numerically on a grid.

Radial functions are solutions of systems of differential equations that define a stationary state of an energy functional for one or more wave-function expansions. It is possible to derive the MCDHF equations from the usual variational procedure by varying both the large and small components so that

$$w_a \begin{bmatrix} V(a;r) & -c\left[\frac{d}{dr} - \frac{\kappa_a}{r}\right] \\ c\left[\frac{d}{dr} + \frac{\kappa_a}{r}\right] & V(a;r) - 2c^2 \end{bmatrix} \begin{bmatrix} P_a(r) \\ Q_a(r) \end{bmatrix}$$

$$= \sum_b \epsilon_{ab}\, \delta_{\kappa_a \kappa_b} \begin{bmatrix} P_b(r) \\ Q_b(r) \end{bmatrix}, \tag{3}$$

where $V(a;r) = V_{\text{nuc}}(r) + Y(a;r) + \bar{X}(a;r)$ is a potential consisting of nuclear, direct, and exchange contributions arising from both diagonal and off-diagonal matrix elements $\langle \Phi_\alpha | \mathcal{H}_{\text{DC}} | \Phi_\beta \rangle$ of the Dirac-Coulomb Hamiltonian [16]. In each κ space, Lagrange related energy parameters $\epsilon_{ab} = \epsilon_{n_a n_b}^\kappa$ are introduced to impose orthonormality constraints in the variational process. In spectrum calculations, where only energy differences relative to the ground state are important, wave functions for a number of targeted states are determined simultaneously in the extended optimal level scheme. This ensures that different eigenstates of the symmetry are orthonormal even though the solutions are approximate. Given initial estimates of the radial functions, the energies E and expansion coefficients $\mathbf{c} = (c_1, \ldots, c_N)^t$ for the targeted states are obtained as solutions to the configuration-interaction (CI) problem

$$\mathbf{Hc} = E\mathbf{c}, \tag{4}$$

where $\mathbf{H}$ is the CI matrix of dimension $N \times N$ with elements

$$H_{ij} = \langle \Phi(\gamma_i \pi J M_J) | H | \Phi(\gamma_j \pi J M_J) \rangle. \tag{5}$$

In GRASP, expansions in terms of CSFs are obtained through single and double (SD) excitations from a multireference (MR) set of CSFs that contain the important contributions to the wave-function composition. In systematic calculations the excitations are to orbital sets of increasing size that include both unfilled and virtual orbitals. Calculations often are classified by their maximum principal quantum number, so an $n = 5$ calculation has associated with it excitations to all orbitals up to $5g$. When the orbital set is increased in size, only the new orbitals need be determined. Expansions may grow

rapidly in size, so partitioning CSFs and omitting interactions between new CSFs can drastically reduce the computation in the self-consistent process.

A GRASP calculation consists of three phases: (i) generating the expansions, (ii) building the orbital basis using variational theory for the Dirac-Coulomb Hamiltonian, and (iii) performing a relativistic configuration-interaction calculation that includes the transverse photon and QED corrections. This process is described in detail in the manual for GRASP2018 [17].

III. LARGE EXPANSIONS

When expansions become exceedingly large, which is the case when millions of small effects (small expansion coefficients) are present, it is useful to partition the set of CSFs according to some criterion to produce a zeroth-order set and a first-order correction, respectively [18]. Suppose the expansion coefficients were vectors $c^{(0)}$ and $c^{(1)}$, respectively. This partitioning also divides the interaction matrix H into blocks so that the eigenvalue problem becomes

$$\begin{pmatrix} H^{(00)} & H^{(01)} \\ H^{(10)} & H^{(11)} \end{pmatrix} \begin{pmatrix} c^{(0)} \\ c^{(1)} \end{pmatrix} = E \begin{pmatrix} c^{(0)} \\ c^{(1)} \end{pmatrix}, \tag{6}$$

where $H^{(00)}$ is the interaction matrix between zeroth-order components, $H^{(11)}$ is for interactions between first-order components of the wave function, and $H^{(01)} = H^{(10)\dagger}$ represents the interactions between CSFs of the two blocks. This equation can be rewritten as a pair of linear equations, namely,

$$(H^{(00)} - EI)c^{(0)} + H^{(01)}c^{(1)} = 0, \tag{7a}$$

$$H^{(10)}c^{(0)} + (H^{(11)} - EI)c^{(1)} = 0. \tag{7b}$$

Solving for $c^{(1)}$ in Eq. (7b) and substituting into (7a), we get an eigenvalue problem for $c^{(0)}$,

$$[H^{(00)} - H^{(01)}(H^{(11)} - EI)^{-1}H^{(10)} - EI]c^{(0)} = 0. \tag{8}$$

This deflates the matrix in that it reduces the eigenvalue problem for a matrix of size $N \times N$ (several million) to an eigenvalue problem of size $m \times m$ (several tens of thousands), where m is the expansion size of $c^{(0)}$. Of course, once E and $c^{(0)}$ have been determined, the other components can be generated from the expression

$$c^{(1)} = -(H^{(11)} - EI)^{-1}H^{(10)}c^{(0)} \tag{9}$$

and a full wave function is defined. Note that the eigenvalue problem is now nonlinear in the eigenvalue that can be solved by an iterative process. When $H^{(11)} - EI$ is replaced by the diagonal matrix such as $H_{ii}^{(11)} - E^0 I$, Eq. (8) is again a linear eigenvalue problem.

In the CI plus many-body perturbation theory (MBPT) approach, referred to as CI+MBPT [19,20], when $c^{(1)}$ is associated with correlation in the core and $c^{(0)}$ with valence correlation, the matrix of Eq. (8) represents the matrix from an effective Hamiltonian. Consequently, interactions between first-order core corrections to the wave function are not included. Thus, contributions to the wave function need to be small. When other atomic properties are evaluated, it would be desirable for $c^{(1)}$ to be sufficiently small so that contributions

TABLE I. Mean radii $\langle r \rangle_{nl}$ (in a_0) of Ce^{2+} orbitals for two configurations $4f^2 5s^2 5p^6$ and $5s^2 5p^6 5d^2$.

|	$\langle r \rangle_{nl}$	
nl	$4f^2 5s^2 5p^6$	$5s^2 5p^6 5d^2$
	$j = l - 1/2 \ (\kappa > 0)$	
$4p_-$	0.659	0.657
$4d_-$	0.745	0.733
$4f_-$	1.152	
$5p_-$	1.752	1.659
$5d_-$		2.408
	$j = l + 1/2 \ (\kappa < 0)$	
$4s$	0.638	0.635
$4p_+$	0.684	0.679
$4d_+$	0.757	0.742
$4f_+$	1.165	
$5s$	1.569	1.504
$5p_+$	1.830	1.727
$5d_+$		2.443

FIG. 1. Large components of $4f_+ = 4f_{7/2}$ (nodeless) and $5p_+ = 5p_{3/2}$ (oscillating) orbitals from the configurations $4f^2 5s^2 5p^6$ (black) and $5s^2 5p^6 5d^2$ [red (gray)].

from the relevant operator *between* small corrections can be omitted.

Partitioning the configuration-interaction matrix so that the CSFs in $c^{(1)}$ space have small coefficients has been supported already in the ATSP code [21], but in variational methods, omitting interactions between these CSFs comes at a cost. The total energy associated with a wave function is an upper bound to the exact energy, but when off-diagonal matrix elements of $H^{(11)}$ are neglected, the total energies often are too low. In the present work, the final relativistic configuration-interaction calculation always included the full matrix but used as many as 96 parallel processors for execution of the task.

Partitioning can also be introduced in the building of an orbital basis. Suppose the $n = 5$ orbitals have already been determined and important contributors to the wave-function composition have been identified. These define $c^{(0)}$. Then the energy functional for the variational process could neglect interactions within the $c^{(1)}$ space, greatly reducing the time to determine orbitals that satisfy orthogonality constraints. Variational methods optimize the orbital basis. The effect on the calculation of neglecting some interactions is a slower rate of convergence of the systematic procedure and an extra layer of orbitals may ultimately be needed. This process was used effectively in the study of Pr^{3+} [9]. In the present study, this option was only used when expansions were large, in which case the $c^{(0)}$ space was defined as the MR set, unless indicated otherwise.

IV. TWO-ELECTRON SYSTEM

A simple Dirac-Hartree-Fock calculation for the ground-state configuration [Xe]$4f^2$ of Ce^{2+} shows that the $4f$ orbitals are not outer orbitals, but orbitals with mean radii between those for {$4s, 4p, 4d$} and {$5s, 5p$} orbitals as shown in Table I. Results are given for two configurations, one with $4f^2$ and the other with $5d^2$. Normally, for a given electron, the nucleus is screened by other electrons with a smaller mean radius. However, Table I shows that when the $4f^2$ electrons are
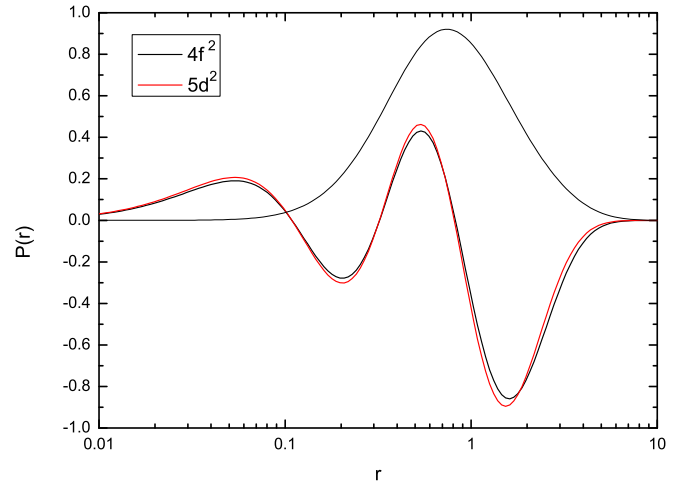
replaced by $5d^2$ electrons, the common orbital parameters hardly change. Figure 1 shows how close to each other the large components of $5p$ orbitals of $4f^2 5s^2 5p^6$ (black line) and $5s^2 5p^6 5d^2$ [red (gray) line] are. Also shown for comparison is the nodeless $4f$ orbital. Because the $4f$ orbital amplitude is so small near the origin, it affects the potential for other electrons only at larger values of the radius.

By expanding the wave function for a two-electron system outside a core through SD excitations to an increasing set of orbitals, the $4f^2$ spectrum converges rapidly as shown in Table II. Because of the strong interaction between $4f^2$ and $5d^2$, radial functions were optimized (equally weighted) for levels of both configurations. For the converged results, the ground-state energy E_g was $-8848.36E_h$. For comparison, the observed energy levels from Ref. [22] are provided as well as the best results reported by Safronova *et al.* [12]. Note, however, that the $^1G_4$ level is not in the observed order.

TABLE II. The $4f^2$ energy levels (in cm^{-1}) from a two-electron calculation compared with observed energy levels [22]. The ground-state energy is $-E_g = 8848.36E_h$. The results from Ref. [12] were calculated using a CI all-order method.

LSJ	$n = 5$	$n = 6$	$n = 7$	$n = 8$	Ref. [22]	Ref. [12]
$^3H_4$	0	0	0	0	0.00	0
$^3H_5$	1246	1250	1249	1251	1528.32	1565
$^3H_6$	2571	2573	2567	2570	3127.10	3227
$^3F_2$	3870	3852	3808	3801	3762.75	
$^3F_3$	4679	4663	4620	4614	4764.76	
$^3F_4$	6399	6267	6206	6181	5006.06	
$^1G_4$	4678	4510	4442	4403	7120.00	7650
$^1D_2$	13639	13316	13175	13103	12835.09	13786
$^3P_0$	17067	16944	16825	16807	16072.04	
$^3P_1$	17485	17368	17253	17237	16523.66	
$^3P_2$	18171	18037	17921	17903	17317.49	
$^1I_6$	19668	19157	19104	19045	17420.60	
$^1S_0$	32006	30967	30512	30362	32838.62	

TABLE III. Wave-function expansion for the largest basis states of the supercomplex. Included are the CSFs, their expansion coefficient, and the excitation producing the CSF.

CSF	Coefficient	Excitation
$4d^{10}5s^25p^6$	0.9734	
$4d^9 4f(^1P)5s^25p^5 5d$	0.0854	$4d5p \rightarrow 4f5d$
$4d^8(^3P)4f^2(^3P)5s^25p^6$	-0.0715	$4d^2\,{}^3P \rightarrow 4f^2\,{}^3P$
$4d^8(^3F)4f^2(^3F)5s^25p^6$	-0.0596	$4d^2\,{}^3F \rightarrow 4f^2\,{}^3F$
$4d^{10}5s^25p^4(^3P)5d^2(^3P)$	-0.0559	$5p^2\,{}^3P \rightarrow 5d^2\,{}^3P$
$\vdots$		
$4d^8(^3P)4f^2(^3P)5s^25p^4(^3P)5d^2(^3P)$	0.0059	$4d^2\,{}^3P \rightarrow 4f^2\,{}^3P$
		$5p^2\,{}^3P \rightarrow 5d^2\,{}^3P$

This first analysis reveals the importance of the mixing of $4f^25s^25p^6$ with $5s^25p^65d^2$.

V. SOME PROPERTIES OF CORRELATION

The lanthanides all have two incomplete shells, namely, the $n = 4$ shell that is missing $4f$ electrons and the $n = 5$ shell missing $5d$, $5f$, and $5g$ electrons. Each of these shells has a complex of configurations that may interact strongly through near degeneracy [23]. Let us consider Ce^{4+} where all subshells are filled. In this case the complexes are defined as $\{4s + 4p + 4d\}^{18} = 4^{18}$ and $\{5s + 5p\}^8 = 5^8$, respectively, where the exponent denotes the number of electrons in a given shell. These two complexes can be merged into a *supercomplex* $4^{18}5^8$. The importance of correlation in the latter can be seen from a study of Ce^{4+}, $4s^24p^64d^{10}5s^25p^6\,{}^1S_0$ where occupied orbitals are excited by the SD process, to unfilled or unoccupied orbitals. Variational calculations yielded a wave-function expansion for which some of the larger basis states in *LSJ* coupling are given in Table III. Of special interest are excitations without a change in the principal quantum number since they represent excitations between near-degenerate states of a complex.

This investigation shows that the largest excitation is $4d5p \rightarrow 4f5d$, namely, a double excitation consisting of single excitations from each of the two complexes. This is followed by $4d^2 \rightarrow 4f^2$ and then $5p^2 \rightarrow 5d^2$ excitations. The above contributions are too large to be considered as a small correction for most applications. Also tested was the effect of adding the quadruple excitations $4d^2LS \rightarrow 4f^2LS$ and $5p^2L'S' \rightarrow 5d^2L'S'$ to the expansion. As shown in Table III, the coefficient for $LS = L'S' = {}^3P$ was 0.0059, which might be important in some circumstances. Contributions to the wave function from $4p^6$ or $4s^2$ are less than 0.0244 and 0.0173, respectively. Notice that all the large excitations within or between complexes did not change their principal quantum number. Ce^{2+} differs in that the $n = 4$ complex 4^{20} now has an extra unfilled subshell $4f^2$ that leads to many states and the analysis is not as simple but the concepts are the same. For Ce^{4+}, the (unnormalized) wave function generated from SD excitations of a supercomplex can be written as

$$\Psi(4^{18}5^8\,{}^1S_0) = [1 + \hat{S}^2(4) + \hat{S}^2(5) + \hat{S}^1(4)\hat{S}^1(5)]$$
$$\Phi(4s^24p^64d^{10} \cdot 5s^25p^6\,{}^1S_0), \quad (10)$$

where $\hat{S}^1(n)$ and $\hat{S}^2(n)$ are the operators performing, respectively, all single and double excitations among the designated nl orbital set and, when applied to the configuration designating the complex, preserve parity and total quantum numbers. Here we have used the fact that $\hat{S}^1(n)$ excitations by themselves are not allowed for ${}^1S_0$ states. The $\hat{S}^1(4)\hat{S}^1(5)$ excitation is a double excitation involving one orbital from each group.

A wave function of the form

$$\Psi(4^{18}5^8\,{}^1S_0) = [1 + \hat{S}^2(4)]\Phi(4s^24p^64d^{10}\,{}^1S_0)$$
$$\times [1 + \hat{S}^2(5)]\Phi(5s^25p^6\,{}^1S_0)$$
$$+ \hat{S}^1(4)\hat{S}^1(5)\Phi(4s^24p^64d^{10} \cdot 5s^25p^6\,{}^1S_0)$$

$$(11)$$

includes also some higher-order terms and would be appropriate when large effects are present in both groups. Here the $\times$ operator represents the vector coupling of CSFs from the left set with those of the right and the required antisymmetrization. Notice that in this form the correlation in the $n = 4$ group is applied to each excitation of the $n = 5$ group. If the size of the expansion is N_4, N_5, and N_{45}, respectively, the number of basis states is $N_4 \times N_5 + N_{45}$. When the expansion for $n = 4$, for example, is fixed, then $N_4 = 1$ and the expansion coefficients that need to be determined may reduce dramatically.

VI. TEN VALENCE ELECTRONS OUTSIDE A $4d^{10}$ CORE

In a GRASP calculation, instead of complexes, the electrons are classified as inactive core, active core, and valence electrons. In this study we treat $4d^{10}$ as an active core and $4f^25s^25p^6$ as ten valence electrons. The $4s^24p^6$ subshells are relegated to the inactive core since the complex study showed that their contribution to the energy was smaller. In these calculations SD excitations were applied to both $4f^25s^25p^6$ and $5s^25p^65d^2$, which define the MR set. Optimization was on all states of $4f^2$ weighted equally, with increasing orbital active sets up to h orbitals but omitting $8h$. Orbital sets for $n = 6$–8 were determined from interactions with the MR set as well as $4f5s^25p^65f$ in order to take into account any possible term dependence when the $4f$ orbitals were optimized separately. The expansions for $n = 8$ were extended to also include excitations from the $4d^{10}$ core of each member of the MR set, expanded to include $4f^25s^25p^45d^2$, in order to estimate the effect of adding some core-core (CC) correlation without any orbital optimization. The CC orbital set was limited to allow only excitations to $4f$, $5d$, and $5f$ orbitals. Results are shown in Table IV.

The results from these $n = 5$ to $n = 8h$ valence-valence (VV) correlation calculations have levels in their correct order. The fine structure for the ${}^3H$ level has improved somewhat. Notice that the total energies have converged except for the highest level, namely, ${}^1S_0$, for which convergence is slower. An investigation of the wave-function composition for $n = 8h$ showed that the $4f^25s^25p^45d^2$ CSF had expansion coefficients larger than 0.09 for the ${}^1S_0$ state. Comparison with the spectrum from the two-electron study (Table II) shows that including correlation for the additional $5s^25p^6$ electrons has not had a large effect on the spectrum but did lower the total

TABLE IV. The $4f^2$ energy levels (in cm^{-1}) from a ten-electron calculation compared with observed energy levels and the ground-state energy (E_g in hartree units). The $n = 8h$ results are extended to include an estimate of the core correlation in +CC.

LSJ	$n = 5$	$n = 6h$	$n = 7h$	$n = 8h$	+CC
$^3H_4$	0	0	0	0	0
$^3H_5$	1400	1452	1464	1467	1619
$^3H_6$	2869	2905	2917	2919	3124
$^3F_2$	4375	4230	4123	4102	3859
$^3F_3$	5231	5092	4994	4976	4800
$^3F_4$	5357	5175	5047	5012	4752
$^1G_4$	7245	7045	6914	6878	6665
$^1D_2$	15130	14597	14232	14107	13522
$^3P_0$	19038	18475	18068	17931	17527
$^3P_1$	19376	18783	18386	18257	17708
$^3P_2$	20006	19377	18986	18859	18238
$^1I_6$	19531	19425	19308	19221	19634
$^1S_0$	40094	37501	36141	35386	33956
$-E_g$	8848.58	8848.65	8848.66	8848.66	8848.82

TABLE V. The $4f^2 5s^2 5p^6$ energy levels (in cm^{-1}) from calculations that include correlation with the $4d^{10}$ active core, compared with observed energy levels [22]. Also reported is the total energy $-E_g$ of the ground state and the number (No.) of CSFs in the expansions. The results from Ref. [12] were calculated using a CI all-order method.

LSJ	$n = 4$	$n = 5$	$n = 6$	$n = 7$	Ref. [22]	Ref. [12]
$^3H_4$	0	0	0	0	0	0
$^3H_5$	1636	1516	1598	1593	1528.32	1565
$^3H_6$	3296	3116	3233	3204	3127.10	3227
$^3F_2$	4685	4250	4305	4299	3762.75	
$^3F_3$	5749	5321	5393	5371	4764.76	
$^3F_4$	7899	5496	5513	5477	5006.06	
$^1G_4$	5680	7542	7620	7555	7120.00	7650
$^1D_2$	16693	15350	15242	15109	12835.09	13786
$^3P_0$	21043	19059	19053	18941	16072.04	
$^3P_1$	21541	19451	19408	19264	16523.66	
$^3P_2$	22411	20138	20118	19953	17317.49	
$^1I_6$	23391	20158	19992	19829	17420.60	
$^1S_0$	41547	40504	39452	38758	32838.62	
$-E_g$	8848.62	8848.85	8849.03	8849.07		
No.	33 520	1 606 947	2 678 670	4 679 330		

energy of the ground state by about 0.30 $E_{\rm h} \approx 66\,000$ cm^{-1}. The largest effect is on the $^1S_0$ level.

VII. CONTRIBUTIONS FROM THE $4d^{10}$ CORE

In the preceding section, $5s^2 5p^6$ was considered to be part of the valence electrons, with relatively small excitation energies. The $4d^{10}$ electrons are different in that the $4d^2 \to 4f^2$ excitation has a large effect on the total energy, although not on the $4f^2$ spectrum.

A. Core-valence correlation

In the supercomplex of Ce^{4+}, a strong effect on the wave-function composition arose from the $4d5p \to 4f5d$ excitation. In our computational method, such interactions are between core and valence electrons and account for the polarization of the $4d^{10}$ core by outer electrons. The Ce^{2+} results are similar. The largest component arises from $4d^9 4f^3 5s^2 5p^5 5d$ and $4d^9 4f 5s^2 5p^5 5d^3$ CSFs, but many are small corrections that could be included as a first-order correction.

B. Properties of core correlation

Core correlation has some special properties in that all subshells are filled and have $^1S_0$ quantum numbers. Though GRASP is fully relativistic, we will discuss this property in the nonrelativistic case.

The SD excitations from the core shells of a CSF consist of all excitations of the type $(ab)\pi LS \to (vv')\pi LS$, where a and b are core orbitals, π designates the parity of the pair of orbitals, and vv' is any pair of unfilled or virtual orbitals. In the case of $4d^{10}$, the pairs can be derived by first uncoupling two equivalent electrons using the coupling relationship

$$|4d^{10}\,^1S\rangle = \sum_{LS} |4d^8\,(LS),\ 4d^2(LS)\rangle(d^8\,LS,\ d^2\,LS|\}d^{10}\,^1S),$$

where $(d^8\,LS,\ d^2\,LS|\}d^{10}\,^1S)$ is a coefficient of fractional grandparentage [24]. The excited CSFs are obtained by the replacement process $4d^2 LS \to nln'l'LS$. The possible LS values for d^2 are $\{^1G, ^3F, ^1D, ^3P, ^1S\}$ and these define the excited pair correlation functions for a correlated core. In the relativistic case, additional quantum numbers are needed as described in [25]. The matrix element for the interaction from this excitation is the *same for all* CSFs, provided the $nln'l'$ orbitals are not present in the valence portion of the CSF. As a result, certain excitations may reduce the total energy (and affect the wave function) significantly but have a minor effect on a spectrum, since the latter is defined as an energy difference relative to the ground state.

Core correlation can be treated as a correction to an atomic state function by correlating the core of all CSFs in the MR set. This may be appropriate when the effect is small, but for cases where the effect is large, the core of every CSF of the valence space should be correlated. One way of doing so is to use an effective Hamiltonian as is done in CI MBPT [19]. In this case core correlation is a first-order correction of the wave function and is applied to all CSFs defining the valence space, including those that are introduced by the SD process. At no point are the interactions between these corrections introduced. A more general approach is given by Eq. (11).

C. Results for an active $4d^{10}$ core

Table V shows some results for calculations that include VV, core-valence (CV), and CC correlation effects on the $4f^2$ spectrum with an active $4d^{10}$ core. Expansions increase in size rapidly, so the orbital set for CC needs to be controlled as well as the MR set. In the $n = 4$ calculation, the MR set included both $4f^2 5s^2 5p^6$ and $5s^2 5p^6 5d^2$ and an orbital set with orbitals up to $\{5s, 5p, 5d, 4f\}$ or simply $\{5554\}$. The inactive core orbitals were the same as those of the two-electron calculation.

Excitations were SD excitations from all shells. Double excitations from $4d^{10}$ were limited to excitations to $\{4f, 5d, 5f\}$ orbitals with the $5g$ orbital participating only in CV and VV in the $n = 5$ calculation with a $\{55555\}$ excitation orbital set. The MR set then also contained $4f5s^25p^65f$, $4f5s^25p^55d^2$, and $5s^25p^45d^4$, although the latter two did not contribute to CC, the number of excitations being too numerous for inclusion. The effect of including CC correlation was the contraction of the $(4f_-, 4f_+)$ orbitals from a mean radius of $(1.174a_0, 1.189a_0)$ to $(1.095a_0, 1.091a_0)$. The fine-structure splitting of the lowest term is now in excellent agreement with observation. The $n = 5$ expansion was reduced by extracting those CSFs with an expansion coefficient greater in magnitude than 0.000 01 in at least one eigenvector. To this were added CSFs from an $n = 6$ expansion including at least one $n = 6$ orbital in a CV-VV expansion from the five members of the MR set. Again, the $n = 6$ results were reduced and $n = 7$ CSFs added to the reduced expansion. The new CSFs have had a small effect on the lower levels but make a significant contribution to higher levels. Note that the ^3P fine structure is in fairly good agreement with observation in that all levels of the latter are shifted by a similar amount. At the same time, comparing the final ground-state energy for the ten-electron system reported in Table IV, the ground-state energy has been lowered by $0.25 E_{\rm h}$ or $54\,869\,{\rm cm}^{-1}$. In other words, correlation shifts the total energies more than it modifies the spectrum. Except for the $^1D_2$ level, the lower levels of the $n = 5$ calculation agree with observation slightly better than the best results reported by Safronova *et al.* [12].

VIII. ANALYSIS

Comparison of computed energy levels with those derived from observation is a common method for assessing the accuracy of a calculation. However, as we have already seen, not all contributions to a wave function affect the computed spectrum. For the prediction of other atomic properties such as lifetimes or transition rates, the accuracy of the wave-function composition is a more important factor. For the analysis of a wave function it is convenient to transform the expansion to *LSJ* coupling [26]. The expansion coefficients depend on the radial basis, but a wave function can also be viewed as a linear combination of multielectron spin-angular functions that are not affected by radial transformations.

Table VI shows how the expansion coefficients for major contributors to the $4f^2\,^1S_0$ wave function change with the correlation model. Given are the coefficients of some CSFs (the contribution to the composition is the square of the coefficient) for the three approximations: the $4f^2$ two-electron system outside inactive closed shells, the $4f^25s^25p^6$ ten-electron system outside closed shells, and finally the $4d^{10}4f^25s^25p^6$ 20-electron system outside closed shells. For the first method, there is strong interaction between $4f^2$ and $5d^2$ partly because the $5d^2$ energy levels overlap those of $4f^2$ and the energy difference of the two is too small. The lowest $5d^2$ level is $^3F_2$ (not included in any table) and its computed energy level is $33\,558\,{\rm cm}^{-1}$ compared with the observed value of $40\,440.20\,{\rm cm}^{-1}$. Including the correlation of $4f^2$ with $5s^25p^6$ increases the separation between the levels and reduces the expansion coefficient. Including also the correlation with $4d^{10}$

TABLE VI. Analysis of the wave-function composition and total energy (in $E_{\rm h}$) for the $4f^2\,^1S_0$ state from the three types of calculations. Included are the expansion coefficient and the CSF when converted to *LSJ* coupling.

Coefficient	CSF
$4f^2\,^1S_0$: $E = -8848.2204$	
0.8522	$4f^2\,^1S_0$
0.4794	$5d^2\,^1S_0$
−0.1351	$4f5f\,^1S_0$
−0.1246	$4f^2\,^3P_0$
−0.0638	$5f^2\,^1S_0$
$4f^25s^25p^6\,^1S_0$: $E = -8848.5021$	
0.9020	$4f^2(^1S)5s^25s^25p^6\,^1S_0$
0.2780	$5s^25p^65d^2\,^1S_0$
−0.0903	$4f^2(^1S)5s^25p^4(^3P)5d^2(^3P)\,^1S_0$
−0.0864	$4f^2(^3P)5s^25p^6\,^3P_0$
−0.0820	$4f^2(^1S)5s^25p^4(^1D)5d^2(^1D)\,^1S_0$
−0.0798	$4f5s^25p^66f\,^1S_0$
−0.0719	$5s^25p^65d6d\,^1S_0$
−0.0696	$4f5s^25p^65f\,^1S_0$
0.0695	$4f^2(^1S)5s^25p^4(^1S)5d^2(^1S)\,^1S_0$
−0.0652	$4f5s^25p^5[^1D]5d^2(^1D)\,^1S_0$
−0.0645	$4f5s^25p^5[^1G]5d^2(^1G)\,^1S_0$
0.0594	$4f^2(^1D)5s[^2D]5p^65d\,^1S_0$
−0.0531	$4f^3(^2F)5s[^3F]5p^5[^2D]5d\,^1S_0$
−0.0455	$4f^3(^2P)5s^25p^5\,^1S_0$
−0.0448	$5s^25p^65f^2(^1S)\,^1S_0$
$4d^{10}4f^25s^25p^6\,^1S_0$: $E = -8848.8937$	
0.9029	$4d^{10}4f^2(^1S)5s^25s^25p^6\,^1S_0$
0.2579	$4d^{10}5s^25p^65d^2\,^1S_0$
−0.1263	$4d^{10}4f5s^25p^65f\,^1S_0$
−0.0865	$4d^{10}4f^2(^3P)5s^25p^6\,^3P_0$
−0.0721	$4d^{10}4f^2(^1S)5s^25p^4(^3P)5d^2(^3P)\,^1S_0$
−0.0667	$4d^{10}4f^2(^1S)5s^25p^4(^1D)5d^2(^1D)\,^1S_0$
−0.0623	$4d^{10}4f5s^25p^5[^1G]5d^2(^1G)\,^1S_0$
0.0610	$4d^94f^3(^2F)[^1P]5s^25p^5[^2D]5d\,^1S_0$
−0.0587	$4d^{10}4f5s^25p^5[^1D]5d^2(^1D)\,^1S_0$
0.0558	$4d^{10}4f^2(^1S)5s^25p^4(^1S)5d^2(^1S)\,^1S_0$
0.0556	$4d^{10}4f5s^25p^66f\,^1S_0$
−0.0478	$4d^8(^3P)4f^4(^3P)[^1S]5s^25p^6\,^1S_0$
0.0474	$4d^{10}4f^2(^1D)5s[^2D]5p^65d\,^1S_0$
0.0462	$4d^8(^1S)4f^4(^1S)5s^25p^6\,^1S_0$

further decreases the contribution to the wave function by a relatively small amount. At the same time, the computed $4d^2\,^3F_2$ energy level is now $63\,429\,{\rm cm}^{-1}$ and hence too high.

Table VI also shows that the core correlation lowers the total energy of the $^1S_0$ level by slightly more than correlation between $4f^2$ and the $5s^25p^6$ closed shells in that the difference in total energies of the state is slightly larger between the last two results than the first two. Because the number of SD excitations from $4d^{10}$ increases extremely rapidly with the size of the excitation orbital set, the present work has limited its size. As in the supercomplex discussed earlier, the largest excitation is $4d5p \to 4f5d$ but with a smaller expansion coefficient, namely, 0.0610 compared with 0.0854 for the complex, as shown in Table III. Similarly, other excitations also have smaller coefficients which may be related

to the presence of the $4f^2$ electrons but may also be the result of correlating the core of only a few CSFs, which has the effect of increasing energy differences and thereby decreasing the expansion coefficients. Further studies are needed.

IX. CONCLUSION

Accurate predictions for lanthanide spectra with multiple open shells provide a challenge for theory. In this work, results were based on the GRASP code that computes a wave function from an MR set along with SD excitations from members of this set, thus including selected higher-order terms and resulting in expansions with millions of basis states.

In effect, correlation is a local phenomenon arising from corrections to the wave from the $\sum 1/r_{ij}$ singularities in the Hamiltonian, but orbitals are global in nature, making the calculations difficult, mainly because of the number of basis states. In Ce^{2+}, ignoring the inactive subshells, there are three correlation regions for which correlation can be computed without difficulty in GRASP, namely, $\Psi(4s^24p^64d^{10}\ ^1S_0)$, $\Psi(4f^2\pi J)$, and $\Psi(5s^25p^6\ ^1S_0)$, where each Ψ is an expansion over CSFs. Then, following the concepts first introduced by Chung [27] and applied successfully to Be-like systems [28], the wave function for Ce^{2+} becomes

$$\Psi(4s^24p^64d^{10}4f^25s^25p^6\pi J)$$
$$= \Psi(4s^24p^64d^{10}\ ^1S_0)\Psi(4f^2\pi J)\Psi(5s^25p^6\ ^1S_0)$$
$$+ \hat{S}_{2o3}\ \Phi(4s^24p^64d^{10}\cdot 4f^2\cdot 5s^25p^6\ \pi J), \qquad (12)$$

where the three individual expansions Ψ are vector coupled and antisymmetrized similarly to the way in which CSFs for a group of subshells are vector coupled. The last term represents the CSF expansion produced by an excitation operator $\hat{S}_{2o3}$ involving at least two of the three subgroups separated by a centered dot. Excluded are excitations for which all excitations are from the same subgroup. This equation is directly related to the equation for generating expansions for a supercomplex, namely, Eq. (11), but here the limitation on excitations has been removed and the equation is not restricted to SD excitation. The fastest rate of convergence for each group would require a different orbital basis for each, leading to a nonorthogonal basis for the full wave function. The present version of GRASP assumes one orthonormal orbital basis leading to larger expansions whose size would be the product of the three sizes. However, this partitioned approach could also provide valuable information about when higher-order excitations such as triple-quadruple excitations are needed.

In the present case, the configuration $4d^84f^45s^25p^45d^2$ is the coupled product of excitations $4d^2 \to 4f^2$ and $5p^2 \to 5d^2$, a special case of a quadruple excitation. From Table VI we see that the largest expansion coefficient in $^1S_0$ is -0.0721 for the $5p^2 \to 5d^2$ excitation whereas the largest coefficient is -0.0478 for the $4d^2 \to 4f^2$ expansion. Depending on the accuracy required for the wave function, the higher-order term may be needed. At the same time, as shown earlier, matrix elements for core correlation may be the same for many CSFs. For example, the CC excitation $4d^2 \to 4f^2$ of a given πJ produces a matrix element for the interaction that is the same for all CSFs that do not already include a $4f$ orbital in their definition. The present code treats each matrix element independently.

A reorganization of the way core correlation is included in GRASP has the possibility of greatly improving the efficiency of the program for lanthanides and other heavy elements.

[1] P. S. Cowperthwaite *et al.*, Astrophys. J. Lett. **848**, L17 (2017).

[2] E. Pian *et al.*, Nature (London) **551**, 67 (2017).

[3] D. Kasen, B. Metzger, J. Barnes, E. Quataert, and E. Ramirez-Ruiz, Nature (London) **551**, 81 (2017).

[4] M. Laatiaoui *et al.*, Nature (London) **538**, 495 (2016).

[5] V. A. Dzuba, V. V. Flambaum, and J. K. Webb, Phys. Rev. A **95**, 062515 (2017).

[6] D. Kasen, N. R. Badnell, and J. Barnes, Astrophys. J. **774**, 25 (2013).

[7] C. J. Fontes, C. L. Fryer, A. L. Hungerford, R. T. Wollaeger, S. Rosswog, and E. Berger, arXiv:1702.02990v1.

[8] M. Tanaka, D. Kato, G. Gaigalas, P. Rynkun, L. Radžiūtė, S. Wanajo, Y. Sekiguchi, N. Nakamura, H. Tanuma, I. Murakami, and H. A. Sakaue, Astrophys. J. **852**, 109 (2018).

[9] C. Froese Fischer and G. Gaigalas, Atoms **8**, 6 (2018).

[10] A. J. Geddes, D. A. Czapski, E. V. Kahl, and J. C. Berengut, Phys. Rev. A **98**, 042508 (2018).

[11] J.-F. Wyart and P. Palmeri, Phys. Scr. **58**, 368 (1998).

[12] M. S. Safronova, U. I. Safronova, and C. W. Clark, Phys. Rev. A **91**, 022504 (2015).

[13] B. Judd, *Operator Techniques in Atomic Spectroscopy* (Princeton University Press, Princeton, 1998).

[14] P. Jönsson, G. Gaigalas, J. Bieroń, C. Froese Fischer, and I. Grant, Comput. Phys. Commun. **184**, 2197 (2013).

[15] C. Froese Fischer, G. Gaigalas, P. Jönsson, and J. Bieroń, Comput. Phys. Commun. **237**, 184 (2019).

[16] C. Froese Fischer, M. Godefroid, T. Brage, P. Jönsson, and G. Gaigalas, J. Phys. B **49**, 182004 (2016).

[17] J. Bieroń, C. Froese Fischer, G. Gaigalas, I. P. Grant, and P. Jönsson, A practical guide to GRASP 2018, 2019, available at http://dx.doi.org/10.17632/x574wpp2vg.1 or https://github.com/compas/grasp2018/releases.

[18] S. Gustafsson, P. Jönsson, C. Froese Fischer, and I. Grant, Atoms **5**, 3 (2017).

[19] M. Kozlov, S. Porsev, M. Safronova, and I. Tupitsyn, Comput. Phys. Commun. **195**, 199 (2015).

[20] V. A. Dzuba, J. C. Berengut, C. Harabati, and V. V. Flambaum, Phys. Rev. A **95**, 012503 (2017).

[21] C. Froese Fischer, G. Tachiev, G. Gaigalas, and M. Godefroid, Comput. Phys. Commun. **176**, 559 (2007).

[22] A. Kramida, Y. Ralchenko, J. Reader, and NIST ASD Team, NIST Atomic Spectra Database, version 5.5.6, available at http://physics.nist.gov/asd (1 September 2018) (National Institute of Standards and Technology, Gaithersburg, 2018).

[23] D. Layzer and J. Bahcall, Ann. Phys. (NY) **17**, 177 (1962).

[24] G. Racah, Phys. Rev. **63**, 367 (1943).

[25] G. Gaigalas, S. Fritzsche, and Z. Rudzikas, At. Data Nucl. Data Tables **76**, 235 (2000).

[26] G. Gaigalas, C. Froese Fischer, P. Rynkun, and P. Jönsson, Atoms **5**, 6 (2017).

[27] K. T. Chung, Phys. Rev. A **44**, 5421 (1991).

[28] K. T. Chung, X.-W. Zhu, and Z.-W. Wang, Phys. Rev. A **47**, 1740 (1993).